Elastodynamic Scattering from a Three-Dimensional Crack in a Fluid-Loaded Halfspace

David E. Budreck

Department of Mathematics and
Dept. of Aerospace Engineering and Engineering Mechanics
Iowa State University
Ames, IA 50011

Ronald A. Roberts

Center for Nondestructive Evaluation
Iowa State University
Ames, IA 50011

Introduction

In this article we present the exact solution of the following canonical problem. We consider the scattering system consisting of a fluid-loaded three-dimensional isotropic elastic halfspace, which is homogeneous except for the presence of a finite flat crack. The crack breaks the surface of the halfspace, and in the current formulation is taken to be orientated normal to the halfspace surface.

The problem is formulated as an integral equation over the face of the crack, using the formalism of Budreck and Achenbach [1]. This is accomplished by using as the kernel of the integral operator the Green's function for a fluid-loaded halfspace developed previously by Roberts [2]. The final result is a matrix which maps incident stress fields to crack-opening displacements, which themselves can be used to compute any field quantities of interest: scattered fields, scattering amplitudes, scattering cross sections, etc.

We note the integral equation formalism is particularly useful in solving scattering problems for which both the scattering system and incident field lack symmetries demanded by other, less universal methods. For the purpose of presenting numerical results we will consider the case of a surface-breaking half-penny-shaped crack under the action of a normally incident two-dimensional (leaky) Rayleigh wave propagating along the halfspace surface. Both frequency and time domain scattered signals will be presented.

This article is structured as follows. In the next section we present the integral equation formulation of the scattering problem. Following that we devote a section to the presentation of both numerical checks (of the numerical code corresponding to the formalism of the previous section), as well as numerical results for the case of Rayleigh wave incidence on a half penny-shaped crack. Finally, we end with a brief summary and conclusion section.

Review of Progress in Quantitative Nondestructive Evaluation, Vol. 11
Edited by D.O. Thompson and D.E. Chimenti, Plenum Press, New York, 1992

Scattering Formalism

In this section we pose the forward scattering problem for a three-dimensional elastic halfspace with fluid loading and a surface-breaking crack. The end result will be an integral equation whose solution constitutes solution of the scattering problem.

Consider first a homogeneous, isotropic, linear elastic, and infinitely extended Cartesian halfspace $V_s \equiv \frac{1}{2}\mathbb{R}^3$ with elastic constant tensor $C^0_{ijk\ell}$ and mass density ρ^0. The elastic halfspace domain is given by $\vec{x} \in V_s$: $\vec{x} \cdot \hat{e}_3 < 0$, here $\hat{e}_3$ is its outward normal where $\hat{e}_i$ denotes a Cartesian basis in $\mathbb{R}^3$. The field equation governing time-dependent wave motion in V_s is

$$\hat{L}^0_{ik}(t, \vec{x}) \left[\hat{u}^0_k(t, \vec{x})\right] = 0, \tag{1}$$

where $\hat{u}^0_k$ is the vector displacement wavefield in the solid and the $\hat{L}^0_{ik}$ operator is given by

$$\hat{L}^0_{ik}(t, \vec{x}) \equiv C^0_{ijk\ell} \partial_{x_j} \partial_{x_\ell} - \rho^0 \delta_{ik} \partial_t^2, \tag{2}$$

and where for our isotropic medium

$$C^0_{ijk\ell} \equiv \lambda^0 \delta_{ij} \delta_{k\ell} + \mu^0 (\delta_{ik} \delta_{j\ell} + \delta_{i\ell} \delta_{jk}). \tag{3}$$

Here $\partial_{x_i} \equiv \partial / \partial x_i$ and $\partial_t \equiv \partial / \partial t$ denote spatial and temporal derivatives, and δ_{ik} is the Kronecker delta. Also the '$\hat{}$' superscript denotes the time-domain Fourier transform of both operator and function in (1). Our Fourier transform convention is

$$\hat{f}(t) = (2\pi)^{-1} \int_{-\infty}^{\infty} d\omega e^{-i\omega t} f(\omega), \quad f(\omega) = \int_{-\infty}^{\infty} dt e^{i\omega t} \hat{f}(t). \tag{4a,b}$$

Application of the transform (4b) to (1) gives

$$L^0_{ik}(\omega, \vec{x}) \left[u^0_k(\omega, \vec{x})\right] = 0, \quad L^0_{ik}(\omega, \vec{x}) \equiv C^0_{ijk\ell} \partial_{x_j} \partial_{x_\ell} + \rho^0 \delta_{ik} \omega^2. \tag{5,6}$$

We further define the corresponding stress field as

$$\sigma^0_{ij}(\omega, \vec{x}) \equiv C^0_{ijk\ell} \partial_{x_\ell} u^0_k(\omega, \vec{x}), \tag{7}$$

with corresponding time domain function $\hat{\sigma}^0_{ij}(t, \vec{x})$ defined as the (4a) transform of the right hand side of (7). We comment that since the final integral equation itself will be solved in the ω-domain, we will continue our formulation in that domain.

In the context of our scattering problem, $\hat{u}^0_k$ will be by definition the incident wavefield. It is itself any wavefield satisfying both the field equation (5) in V_s and the boundary conditions on ∂V:

$$\sigma^0_{3j}(\omega, \vec{x}) = B^s_j(\omega, \vec{x}) \left[p^0(\omega, \vec{x})\right], \quad u^0_3(\omega, \vec{x}) = B^d_3(\omega, \vec{x}) \left[p^0(\omega, \vec{x})\right]. \tag{8a,b}$$

Here $p^0(\omega, \vec{x})$ is the excess pressure in the fluid halfspace $V_f \equiv \mathbb{R}^3 - V_s$ with compressional modulus λ_f and mass density ρ_f, satisfying both (8) on ∂V and the field equation

$$L^f(\omega, \vec{x}) \left[p^0(\omega, \vec{x})\right] = 0, \quad L^f(\omega, \vec{x}) \equiv (\lambda_f) \partial_{x_i} \partial_{x_i} + (\rho_f) \omega^2 \tag{9,10}$$

in V_f. The operators in (8) are those which demand continuity of normal surface traction and displacement, they are

$$B_j^s(\omega,\vec{x}) \equiv -\delta_{3j} \ , \quad B_3^d(\omega,\vec{x}) \equiv -\left((\rho_f)\omega^2\right)^{-1} \partial_{x_3} \ . \tag{11a,b}$$

Consider next the interaction of the incident wavefield with the surface-breaking crack. This gives rise to the scattered displacement wavefield $u_k^{sc}(\omega,\vec{x})$, and the total wavefield everywhere in V_s is given by

$$u_k(\omega,\vec{x}) \equiv u_k^{sc}(\omega,\vec{x}) + u_k^0(\omega,\vec{x}) \ , \tag{12}$$

the corresponding total stress field in V_s is given by

$$\sigma_{ij}(\omega,\vec{x}) \equiv C_{ijk\ell}^0 \partial_{x_\ell} u_k(\omega,\vec{x}) \ . \tag{13}$$

Like the indicent field the total field satisfies everywhere in V_s the field equation

$$L_{ik}^0(\omega,\vec{x})\left[u_k(\omega,\vec{x})\right] = 0 \tag{14}$$

together with boundary conditions on ∂V

$$\sigma_{3j}(\omega,\vec{x}) = B_j^s(\omega,\vec{x})\left[p(\omega,\vec{x})\right] \ , \quad u_3(\omega,\vec{x}) = B_3^d(\omega,\vec{x})\left[p(\omega,\vec{x})\right] \ . \tag{15a,b}$$

Here $p(\omega,\vec{x})$ is the total excess pressure in the fluid halfspace V_f, satisfying both (15) on ∂V and the field equation $L^f p = 0$ in V_f.

The crack surface S, which is taken to be a finite planar surface normally intersecting the halfspace surface ∂V, has for $\vec{x} \in S$ the traction-free boundary condition

$$\sigma_{ij}(\omega,\vec{x})\hat{n}_j(\vec{x}) = 0 \ , \tag{16}$$

here $\hat{n}_j$ is the (arbitrarily chosen of two) normal to the (open) surface S.

Key to the solution of the scattering problem will be the use of the Green's function for the fluid- loaded halfspace. We define this Green's function as that which satisfies the distributional equality

$$L_{ik}^0(\omega,\vec{x})\left[G_k^m(\omega,\vec{x},\vec{z})\right] \equiv -\delta_{im}\delta(\vec{x}-\vec{z}) \tag{17}$$

for $\vec{x}$ and $\vec{z}$ in the solid V_s, together with the boundary conditions

$$D_{3j}^m(\omega,\vec{x},\vec{z}) = B_j^s(\omega,\vec{x})\left[p^g(\omega,\vec{x})\right] \ , \quad G_3^m(\omega,\vec{x},\vec{z}) = B_3^d(\omega,\vec{x})\left[p^g(\omega,\vec{x})\right] \ , \tag{18a,b}$$

for $\vec{x} \in \partial V$, and the causal condition

$$\hat{G}_k^m(t,\vec{x},\vec{z}) = 0, \qquad t < 0 \tag{19}$$

for $\vec{x}$ and $\vec{z}$ in V_s. In (18a) above we are making use of the definition

$$D_{ij}^m(\omega,\vec{x},\vec{z}) \equiv C_{ijk\ell}^0 \partial_{x_\ell} G_k^m(\omega,\vec{x},\vec{z}) \ , \tag{20}$$

and in (19) the $\hat{G}_k^m$ is defined to be the Fourier transform of G_k^m, via (4a). Furthermore, $p^g(\omega,\vec{x})$ is that which satisfies both (18) on ∂V and $L^f p^g = 0$ in V_f. Hence p^g corresponds physically to the excess fluid pressure field due to a point

load in the solid. We comment that the physics of $G_k^m(\omega, \vec{x}, \vec{z})$ is that of a displacement at $\vec{x}$ in the k-direction due to a time harmonic point load of unit amplitude applied at $\vec{z}$ in the m-direction. The $D_{ij}^m(\omega, \vec{x}, \vec{z})$ is thus the corresponding stress at $\vec{x}$ due to the same point load. We will find it convenient to adopt the notation

$$D_m^{ij}(\omega, \vec{x}, \vec{z}) \equiv C_{ijk\ell}^0 \partial_{z_\ell} G_m^k(\omega, \vec{x}, \vec{z}) \tag{21}$$

which is the stress at $\vec{z}$ due to a point load in the m-direction at $\vec{x}$. Here we have used the well-known symmetry condition

$$G_k^m(\omega, \vec{x}, \vec{z}) = G_m^k(\omega, \vec{z}, \vec{x}), \tag{22}$$

and which together with (20) and (21) implies

$$D_{ij}^m(\omega, \vec{x}, \vec{z}) = D_m^{ij}(\omega, \vec{z}, \vec{x}). \tag{23}$$

At this point we have all the necessary pieces with which to construct the integral equation that will subsequently be solved for crack-opening displacement. Its derivation follows the standard application of the divergence theorem to the elastodynamic Betti-Rayleigh reciprocal relation, here for the elastodynamic states u_k^0 and G_k^m corresponding to the incident and fluid-loaded half-space point load response fields. Subsequent to an application of the boundary (18) and causal (19) conditions, we obtain for $\vec{x} \in V_s$

$$u_p^{sc}(\omega, \vec{x}) = \int_S d^2\vec{z} D_p^{ij}(\omega, \vec{x}, \vec{z}) \Delta u_i(\omega, \vec{z}) \hat{n}_j(\vec{z}) \ . \tag{24}$$

Here S is the crack surface satisfying (16) with normal $\hat{n}_j$, and Δu_i is the crack-opening displacement

$$\Delta u_i(\omega, \vec{z}) \equiv u_i(\omega, \vec{z}^+) - u_i(\omega, \vec{z}^-) \ . \tag{25}$$

The convention adopted in (24)–(25) is that for $\vec{z}$ on the crack surface S with normal $\hat{n}_j(\vec{z})$ we have $\vec{z}^\pm = \vec{z}$ denoting the two sides of the physical crack with outward normals $\hat{n}_j(\vec{z}^\pm) = \pm \hat{n}_j(\vec{z})$.

Operating through both sides of (24) by the Hookean operator $C_{\ell mpn}\partial_{x_n}$ gives, again for $\vec{x} \in V_s$,

$$\sigma_{\ell m}^{sc}(\omega, \vec{x}) = C_{\ell mpn}^0 \int_S d^2\vec{z} D_{p,n}^{ij}(\omega, \vec{x}, \vec{z}) \Delta u_i(\omega, \vec{z}) \hat{n}_j(\vec{z}). \tag{26}$$

Taking $\vec{x} \to S$ and subsequently operating through by $\hat{n}_m(\vec{x})$ gives the desired integral equation, it is

$$-\sigma_{\ell m}^0(\omega, \vec{x}) \hat{n}_m(\vec{x}) = C_{\ell mpn}^0 \hat{n}_m(\vec{x}) \int_S d^2\vec{z} D_{p,n}^{ij}(\omega, \vec{x}, \vec{z}) \Delta u_i(\omega, \vec{z}) \hat{n}_j(\vec{z}) \ , \tag{27}$$

which holds $\forall \vec{x} \in S$ and where we have used definitions (7), (12), (13) together with the boundary condition (16).

Equation (27) is the main analytical result of this article. It is a distributional equality which maps the unknown crack opening displacement to the known incident stress field. That the mapping takes place entirely on the crack

surface S is a most desireable property of the integral equation, and is made possible by the availability of the Green's function for a fluid-loaded elastic halfspace.

The integral equations (27) are solved essentially by inverting the integral operator, a process that is complicated by the need to first regularize it, thereby converting a distributional to a pointwise equality. For this purpose the methodology of [1] developed originally for the scattering of cracks in a fullspace applies equally well to (27). The integral equations (27) are solved by successively employing, in the manner of [1], the following steps: (1) Discretization (converts the integral oprator to a matrix operator), (2) Regularization (converts all distributional equalities to pointwise equalities), and (3) Inversion (matrix inversion of the discretized integral equation). The end result is a matrix with components $H_{\alpha\beta}$ satisfying

$$(\Delta u)_\alpha = [H_{\alpha\beta}](\sigma^0)_\beta \ , \tag{28}$$

hence H maps incident stress fields on S to crack-opening displacements. Since in [1] there is one crack-opening displacement component associated with each of N crack elements, H is a $3N \times 3N$ matrix. We note that this involves assuming a constant crack-opening displacement over all elements except those which share a border with the curved crack edge. Over those elements the correct $\sqrt{r}$ asymptotics (operationally, r is the distance from a quadrature point to the crack edge) is built in via a nonuniform shape function, yet in the current formulation no attempt was made to build in the correct asymptotics for those crack elements sharing a border with both the curved crack edge and the flat halfspace surface.

Numerical Results

In this section we present results corresponding to the numerical solution (28) of the integral equation (27). We consider the case of scattering from a normal half penny-shaped crack of radius a, and all frequency domain results will be presented with respect to the dimensionless shear wavenumber $k_T a$. The solid is taken to be aluminum (longitudinal, shear, and traction-free Rayleigh wave velocities are $c_L = 6320$, $c_T = 3080$, $c_R = 2920$m/s), and the fluid is taken first to be air (wavespeed $c_f \equiv \sqrt{(\lambda_f)/(\rho_f)} = 171$m/s) and then water ($c_f = 1485$m/s). The fluid to solid density ratios for these two respective cases were taken to be $1:1000$ and $1:3.25$.

Since we are intersted in solving the scattering problem of a fluid-loaded elastic halfspace containing a surface breaking crack, we will refer to this current model as "exact". For the purpose of comparison we introduce two previously developed models which will here be used to approximate the exact model. The first model will be referred to as the "halfspace approximation", and consists of the model developed by Budreck and Achenbach [3] for a surface-breaking crack in a traction-free halfspace. The approximate nature of this model is due to the use of the fullspace Green's function in the integral equation formalism, but where the traction free halfspace surface was partially taken into account by including in the domain of the integral equation the halfspace surface in the vicinity of the crack mouth. Hence the halfspace approximation model should perform best at low frequencies, yet even at zero frequency is only an approximation. The second model will be referred to as the "fullspace approximation", and consists of using the code developed in [1] for the case of a half penny-shaped crack in a fullspace; the traction-free boundary conditions not being taken into account at all.

In Table I we demonstrate the convergence of the halfspace approximation model to the exact model (run with air loading) for the former being run

with successively larger regions R of discretization of the halfspace surface. The regions R are circular and are centered at the center of the crack mouth. Indicated in the left column of Table I are the various radii of this region R in terms of multiples of the radius 'a' of the crack. Hence the first row of Table I is actually a fullspace approximation comparison. Theoretically, the halfspace approximation model with region R of radius Na should converge to the exact model as $N \to \infty$.

All Table I results were run for a dimensionless shear wavenumber of unity, i.e. $k_T a = 1$. The percent error values were obtained by computing an average percent difference between each element of the halfspace approximation to that of the exact H-matrix elements (28), weighted with respect to the norm of the exact H-matrix element. Space restrictions do not permit a more exacting explanation of this comparison formalism, but we comment that this comparison formalism seems to be a rather severe test of accuracy: In the process of integration required in computing an actual field variable the percent error has been seen to be about a factor of 10 less (as shown later by Fig. 1) than those shown in this (and the following) table.

In Table II we demonstrate a different variation on the same percent error parameter presented in Table I. Here we fix the surface of discretization of the halfspace approximation model to a region R with radius $3a$, and vary the dimensionless shear wavenumber $k_T a$. For $k_T a = 1.5$ we note that the dimensionless shear wavenumber corresponding to the region R is already as high as $1/2$, and hence R will begin to act more like a scatterer and less like a traction free halfspace surface.

In the remaining results we present normalized Auld voltages, see [4]

$$\delta\Gamma(\omega) \equiv \int_S d^2\vec{z}\sigma^0_{ij}(\omega,\vec{z})\Delta u_i(\omega,\vec{z})\hat{n}_j(\vec{z}) \tag{29}$$

due to Rayleigh wave incidence of the crack. We consider a two-dimensional time-harmonic ($O(\omega)$ in displacement) wavefield impinging normally on the

Table I. Convergence of halfspace approximation model to exact model for increasing size of region R, $k_T a$ fixed at 1.

Radius of region R	Error of halfspace approximation model vs. exact model
0	50.8%
a	20.1%
$2a$	11.8%
$3a$	8.9%

Table II. Comparison of halfspace approximation model to exact model for increasing $k_T a$, radius of region R fixed at 3a.

$k_T a$	Error of halfspace approximation model vs. exact model
0.25	7.42%
0.50	8.02%
0.75	8.93%
1.00	8.85%
1.25	8.02%

surface-breaking crack. We plot the normalized Auld voltages $\delta\Gamma$ in both the frequency and time domain. For the time domain plots we use the Fourier transform (4a) to compute the response to a Gaussian pulse which in the frequency domain is centered at zero with an amplitude of unity, and drops to a value of .001 at $k_T a = 6$.

In Figure 1 we plot the frequency domain response of the exact model (run with air loading) for $0 \leq k_T a \leq 1.25$, against which we compare the halfspace approximation response. Note that as mentioned in the discussion of the Table I results we see a much closer comparison of the field quantity $\delta\Gamma$ than was suggested by the Table I results themselves. Again, Table I compared the matrices which, via (28), gives rise to the crack-opening displacements. These are then integrated in (29) to give rise to the result depicted in Fig. 1.

Figures 2–6 all deal with the exact model run for the case of water loading of the halfspace surface. In Figure 2 we plot the norm of the frequency domain response of the exact model for $0 \leq k_T a \leq 6$ with comparison to the fullspace approximation. We comment that it becomes unfeasable to run the halfspace approximation for $k_T a$ much larger than unity, the required increase in the region R quickly puts the code outside the bounds of available computer memory. The fullspace comparison is especially interesting in light of Figure 3: Here we plot the full complex response of the exact and fullspace approximation models.

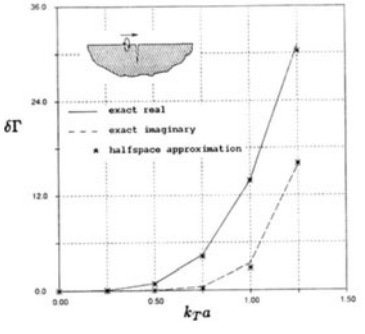

Fig. 1. Complex frequency domain Auld response for Rayleigh wave incidence of exact model with air loading vs. halfspace approximation.

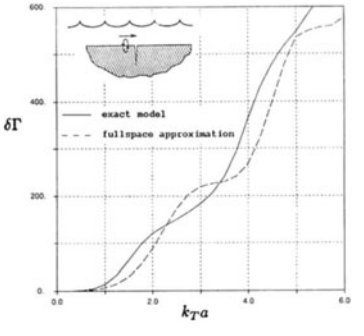

Fig. 2. Norm of frequency domain Auld response for Rayleigh wave incidence of exact model with water loading vs. fullspace approximation.

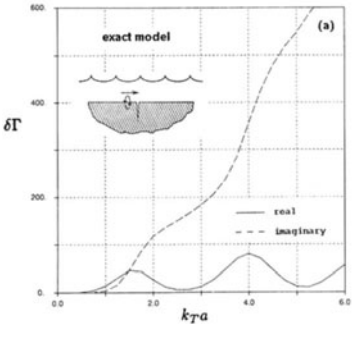

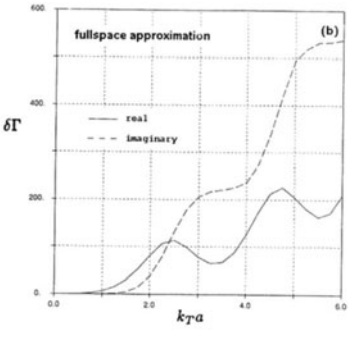

Fig. 3. Complex frequency domain Auld response for Rayleigh wave incidence using (a) Exact model with water loading, (b) Fullspace approximation.

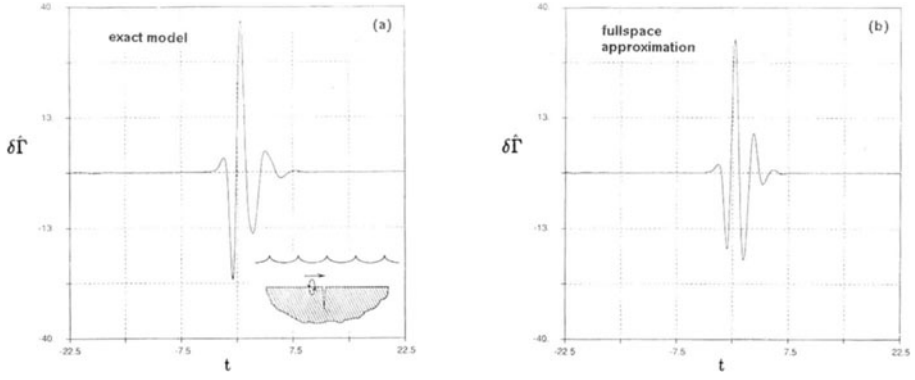

Fig. 4. Time domain Auld response corresponding to Fig. 3 for an incident Gaussian pulse.

Hence we see the fullspace approximation does rather well in getting the norm of the complex response right, but is lacking the proper phase information.

Finally, in Figure 4 we plot the time domain response (normalized Auld voltage) to the aforementioned Gaussian pulse by using (4a) and the corresponding frequency response of Figure 3.

Conclusions

We have exactly solved the canonical problem of scattering from a surface-breaking crack in a fluid-loaded elastic halfspace. This was accomplished by combining the integral equation formalism of Budreck and Achenbach [1] with the fluid-loaded elastic halfspace Green's function of Roberts [2]. The end result is a computer code which generates a matrix that maps, at a given frequency, incident stress fields to crack-opening displacements on the crack surface S. The code was shown to compare well with an approximate model developed previously by Budreck and Achenbach [3]. Numerical results were presented for the case of Rayleigh wave scattering. It was noted that a rather crude fullspace approximation modelled the magnitude of the response quite well, but not the phase. This observation, if it remains relatively invariant with respect to the type of incident field involved, will be key in guiding the development of a second generation approximation model.

Acknowledgements

This work was supported by NIST under cooperative agreement #70NANB9H0916 and was performed at the Center for NDE, Iowa State University.

References

1. Budreck, D. E. and J. D. Achenbach (1988), "Three Dimensional Scattering from Planar Cracks by Boundary Integral Equations Methods," J. Appl. Mech. 55, 405–412.
2. Roberts, R. A. (1990) "Elastodynamic Response of Contacting Fluid and Solid Half-Spaces to a Three-Dimensional Point Load", Wave Motion 12, 583–593.
3. Budreck, D. E. and J. D. Achenbach (1989) "3-D Elastic Wave Scattering by Surface- Breaking Cracks," J. Acoust. Soc. Am. 86, 395–406.
4. Auld, B. A. (1979) "General Electromechanical Reciprocity Relations Applied to the Calculation of Elastic Wave Scattering Coefficients", Wave Motion 1, 3–10.